

## INFLUENCE OF $\text{Sm}_2\text{O}_3$ ADDITION ON DIELECTRIC PROPERTIES OF $\text{BaTi}_{0.95}\text{Sn}_{0.05}\text{O}_3$ CERAMICS

R. ZHAO, Y. LI<sup>\*</sup>, Z. ZHENG, W. KANG, Y. WANG, W. DUN

*Key Laboratory of Environment Functional Materials of Tangshan City, Hebei Provincial Key Laboratory of Inorganic Nonmetallic Materials, College of Materials Science and Engineering, North China University of Science and Technology, Tangshan 063210, Hebei*

Ceramic samples of  $\text{BaTi}_{0.95}\text{Sn}_{0.05}\text{O}_3$  (BTS) were prepared by the conventional solid-state method, and the influence of different doping amounts of  $\text{Sm}_2\text{O}_3$  addition on phase composition, microstructure and dielectric properties of BTS ceramics were investigated. From the XRD patterns, the results show that all samples exhibited pure perovskite phase with no impurity phase, which suggested that  $\text{Sm}^{3+}$  can be dissolved in the BTS to form a uniform solid solution. A small amount of doped  $\text{Sm}_2\text{O}_3$  can refine grains to a certain extent and improve the density of the ceramic body, which is beneficial to improve the dielectric properties of the samples. In a small amount of doping,  $\text{Sm}^{3+}$  first enters the A-site of the BTS ceramic to replace  $\text{Ba}^{2+}$ , causing lattice distortion due to internal stress and increasing the dielectric constant. The samples have the highest dielectric constant ( $\epsilon = 3508$ ) and the lower dielectric loss ( $\tan\delta = 0.018$ ) at a sintering temperature of  $1330^\circ\text{C}$  with 0.4 mol%  $\text{Sm}^{3+}$  doping, showing excellent dielectric properties. Appropriate amount of doped  $\text{Sm}_2\text{O}_3$  also has a certain peak lift, so that the dielectric peak of ceramic samples increased, but the Curie peak shift is not obvious.

(Received January 31, 2018; Accepted September 1, 2018)

*Keywords:*  $\text{BaTi}_{0.95}\text{Sn}_{0.05}\text{O}_3$ ;  $\text{Sm}_2\text{O}_3$ ; doping; dielectric property

### 1. Introduction

Capacitors are widely used in electrical and electronic products [1]. For several decades, lead oxide based ferroelectrics have been widely used in capacitors for their excellent dielectric properties. However, the volatile  $\text{PbO}$  vapor in the process can cause serious environmental pollution [2]. In recent years, ceramics with high permittivity have attracted much attention in the development of environment friendly capacitors [3]. One of the most widely studied perovskite ( $\text{ABO}_3$  structure) ferroelectric oxide is barium titanate ( $\text{BaTiO}_3$ ), whose excellent dielectric and ferroelectric properties are exploited in various electronic devices as capacitors, thermistors, transducers and nonvolatile memories in microelectronic industry. The performance of barium titanate ceramics are prevalently dependent on parameters like: grain size, density, impurities and structural defects [4]. The dielectric constant of barium titanate can be improved by doping Zr [5], Hf [6], Ce [7], Y [8] and Sn [9] with higher permittivity. And the solid solution after doping is environmentally friendly dielectric. Therefore, a possible alternative as capacitor material are the heterovalent B-doped  $\text{BaTiO}_3$  substitutions as  $\text{BaZr}_x\text{Ti}_{1-x}\text{O}_3$  (BZT),  $\text{BaSn}_x\text{Ti}_{1-x}\text{O}_3$  (BTS) and others [10]. Barium titanate doped with Sn shows excellent dielectric properties, with high permittivity, even higher than that of Zr-doped  $\text{BaTiO}_3$  [10, 11]. The permittivity of BZT is not as high as found in BTS at room temperature, which seems to be a valuable candidate for high permittivity applications. BTS was also considered as the replacement of  $\text{BaSrTiO}_3$  as one of the most promising candidate as a microwave dielectric [12].  $\text{BaTiO}_3$  introduced  $\text{Sn}^{4+}$  at B-site to replace  $\text{Ti}^{4+}$ . Since the radius of  $\text{Sn}^{4+}$  (0.069 nm) is larger than the radius of  $\text{Ti}^{4+}$  (0.061 nm), the chemical stability of  $\text{Sn}^{4+}$  is better than that of  $\text{Ti}^{4+}$ . Further, the Curie temperature of the barium tin titanate

<sup>\*</sup> Corresponding author: : lylll2004@126.com

decreased, and the permittivity remarkably increased. At the same time, the perovskite structure is not damaged. In order to meet the needs of different application areas, the researchers doped by various rare earth element to modify, and produced electronic devices<sup>[13,14]</sup> by the standard of X7R (-55~200°C,  $\Delta\epsilon/\epsilon \leq 15\%$ ). Aliovalent doping mechanisms and substitution preferences of trivalent ions in BTS and BaTiO<sub>3</sub> ceramics have been debated for many years because of the intermediate size and charge of the trivalent ions compared with Ba<sup>2+</sup>, Sn<sup>4+</sup> and Ti<sup>4+</sup> ions<sup>[15]</sup>. In this paper, BaTi<sub>0.95</sub>Sn<sub>0.05</sub>O<sub>3</sub>-based ceramic materials as the research object, Sm<sub>2</sub>O<sub>3</sub> as a dopant to explore the morphology and dielectric properties of the samples, and its influence mechanism was analyzed.

## 2. Experimental

BaTi<sub>0.95</sub>Sn<sub>0.05</sub>O<sub>3</sub>+xSm<sub>2</sub>O<sub>3</sub> ceramics was synthesized by the traditional solid-state method using pure BaCO<sub>3</sub>, TiO<sub>2</sub>, SnO<sub>2</sub> and Sm<sub>2</sub>O<sub>3</sub> where x (Sm<sub>2</sub>O<sub>3</sub>) = 0, 0.2%, 0.4%, 0.6%, 0.8% and 1.0%. According to the formula calculation results weighed BaCO<sub>3</sub>, SnO<sub>2</sub>, and TiO<sub>2</sub> into ball grinder to ball mill for 4h and the first material and water with proportion of 1: 2; Then we can obtain BaTi<sub>0.95</sub>Sn<sub>0.05</sub>O<sub>3</sub> ceramic powders after the dried powders were calcined at 1090°C for 2h. After that, The pre-synthesized BTS powders Sm<sub>2</sub>O<sub>3</sub> and water were mixed according to the formula and re-milled for 6 h. The proportion of the secondary material and water was 1: 1.5. The reground, dried powders were added with 5wt.% polyvinyl alcohol (PVA) as a binder for granulation. The granulated powders were sieved through 40-mesh screen and then pressed into pellets of 13mm in diameter and 2mm in thickness under 60 MPa. Sintering was conducted in air at 1280~1330°C for 2 h. The silver paste was painted on both sides as electrodes to provide ohmic contacts after the sintered samples were ultrasonically cleaned in distilled water. Finally the painted samples were fired at 550 °C for 10 min. The samples were left for 24 hours before performance test.

The morphologies of the sintered samples were performed and analyzed with field emission scanning electron microscopy of Japan Hitachi S-4800 cold field emission scanning electron microscopy (SEM). The microstructural phase of the sample was probed by the CuK $\alpha$  target X-ray diffraction (XRD, Rigaku D/max 2500V/pc) from Japan Science and Technology. The capacitance *C* and dielectric loss (tan $\delta$ ) of ceramic bodies were tested with Automatic LCR Meter 4425 at 1 kHz. And the dielectric constant and dielectric loss of the sample are calculated by the following equation. (1), (2):

$$\epsilon = \frac{144 \times C \times h}{\phi^2} \quad (1)$$

$$\tan \delta = \frac{f \times D}{1000} \quad (2)$$

In the formula: *h*—the thickness of the sample (mm);  $\Phi$ —the electrode diameter of the sample (mm); *C*—the capacitance of the sample (pF); *f*—test frequency; *D*—Dielectric loss factor

## 3. Results and discussions

Fig.1 shows the XRD patterns of the Sm<sub>2</sub>O<sub>3</sub>-doped BaTi<sub>0.95</sub>Sn<sub>0.05</sub>O<sub>3</sub> ceramics sintered at 1330 °C for 2h. It can be seen from Fig.1 that there is no secondary phase is detected even for the doping content of Sm<sub>2</sub>O<sub>3</sub> upto 1.0 wt.%, and the all the BTS ceramic sample display a desired perovskite structure. Sn<sup>4+</sup> can be infinitely soluble in BaTiO<sub>3</sub> crystals, and occupying the same position as Ti. In order to further study the influence of doped Sm<sub>2</sub>O<sub>3</sub> on the diffraction peak, the (100) crystal plane in the diffraction pattern is partially enlarged. It can be clearly seen from the Fig.1 that as the doping amount increases, the diffraction peak of the (100) crystal face gradually moves to a high angle and then moves to a lower angle. When the doping amount is 0.4%, it could

reach the maximum angle of  $22.3^\circ$ . The reason for this phenomenon may be related to the substitution of  $\text{Sm}^{3+}$  in BTS. When added a small amount of  $\text{Sm}_2\text{O}_3$ ,  $\text{Sm}^{3+}$  enters into the A-site to replace  $\text{Ba}^{2+}$ , because the radius of  $\text{Sm}^{3+}$  is less than  $\text{Ba}^{2+}$ , the lattice distortion occurs after substitution, the lattice constant becomes smaller and the diffraction angle shifts to the right. As the doping amount of  $\text{Sm}_2\text{O}_3$  further increases,  $\text{Ti}^{4+}$  is replaced by  $\text{Sm}^{3+}$  in B-site. Since the radius of  $\text{Sm}^{3+}$  is larger than that of  $\text{Ti}^{4+}$ , the diffraction angle shifts to the left. Different doping levels of  $\text{Sm}_2\text{O}_3$  lead to changes in the internal structure of the sample crystal, and this change also affects the various properties of the sample.

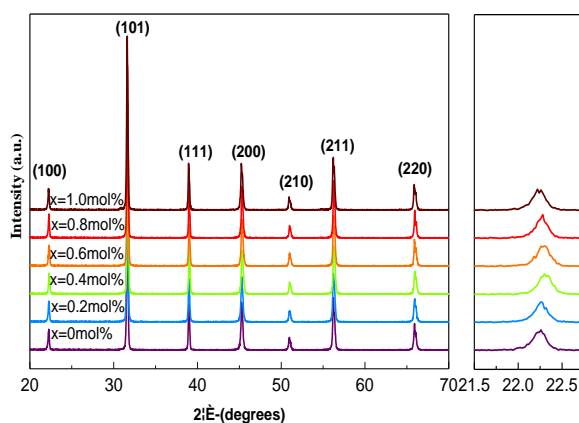


Fig.1. XRD patterns of  $\text{Sm}_2\text{O}_3$ -doped BTS ceramics prepared at  $1300^\circ\text{C}$  for 2 h.

The ionic radius of  $\text{O}^{2-}$  is 0.140 nm, the radius of  $\text{Ti}^{4+}$  is 0.061 nm, the radius of  $\text{Ba}^{2+}$  is 0.161 nm, and the radius of  $\text{Sm}^{3+}$  is 0.096 nm. According to the tolerance factor calculation, as shown in equation (3), the tolerance factor ( $t$ ) of  $\text{Sm}^{3+}$ -doped BTS is shown in Table 1. As can be seen from Table 1, after  $\text{Sm}^{3+}$  enters the interior of the crystal lattice, it can replace the A-site or the B-site.

$$t = \frac{(r_A + r_O)}{\sqrt{2}(r_B + r_O)} \quad (3)$$

In the equation:  $t$  is the tolerance factor,  $r_A$  is the ion radius of A-site,  $r_B$  is the ion radius of B-site, and  $r_O$  is the radius of  $\text{O}^{2-}$  ion.

Table 1.  $\text{Sm}^{3+}$ -doped BST tolerance factor.

Replace the location	$t$
A-site $\text{BaTiO}_3$	0.83
A-site $\text{BaSnO}_3$	0.80
B-site $\text{BaSnO}_3$ Or $\text{BaTiO}_3$	0.90

Fig. 2 (a)~(f) illustrates the micrographs of BTS ceramics with various  $\text{Sm}_2\text{O}_3$  contents by SEM. It can be seen from the Fig. 2 that all the ceramic samples have a clear grain boundary. Compared with 0-doped (a), the grain size was obviously refined and the density of grains increased obviously when the BTS ceramics were doped with 0.2wt.% and 0.4wt.%  $\text{Sm}_2\text{O}_3$ . It may be due to  $\text{Sm}^{3+}$  accumulating at grain boundaries and acting as a pinning grain boundary and suppressing grain growth of the main crystal phase [16], resulting in a decrease in grain size.  $\text{Sm}^{3+}$  first enters the A-site to be replaced. Since the radius of  $\text{Sm}^{3+}$  is smaller than the radius of  $\text{Ba}^{2+}$ , it

will lead to the lattice shrinkage, the reduction of the cell constant, the density increases, which is conducive to the increase of the dielectric constant. With the further increase of doping amount, the grain size increases and the porosity increases. The porosity obviously increases when the doping amount of  $x(\text{Sm}_2\text{O}_3) = 1.0\%$ . The increase in porosity can be detrimental to the dielectric properties of the sample. The macroscopic dielectric properties of the sample may be affected by these microscopic structural changes.

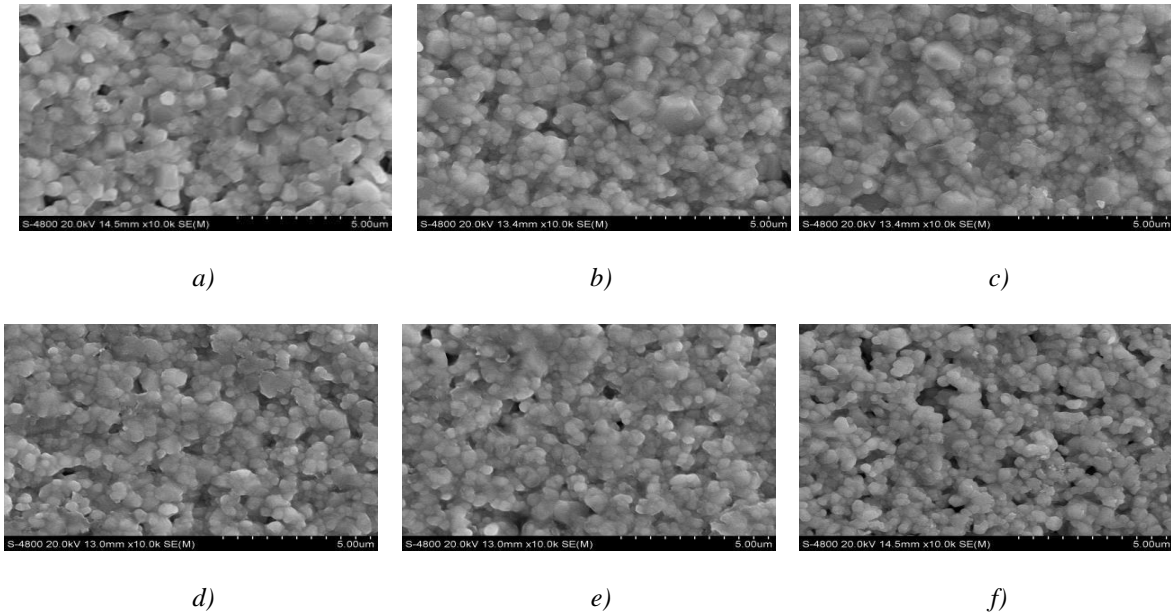


Fig. 2. SEM images of BTS sintered at 1330 °C for 2h: (a)  $x = 0\text{mol}\%$ , (b)  $x = 0.2\text{mol}\%$ , (c)  $x = 0.4\text{mol}\%$ , (d)  $x = 0.6\text{mol}\%$ , (e)  $x = 0.8\text{mol}\%$ , (f)  $x = 1.0\text{mol}\%$ .

Fig. 3 and Fig. 4 shows that dielectric constant and dielectric loss of BTS ceramics doping with  $\text{Sm}_2\text{O}_3$  as  $0\text{mol}\%$ ,  $0.2\text{mol}\%$ ,  $0.4\text{mol}\%$ ,  $0.6\text{mol}\%$ ,  $0.8\text{mol}\%$  and  $1.0\text{mol}\%$  at the frequency of 1 kHz at different temperatures.

As shown in Fig.3, the dielectric constant of the samples sintered at different temperatures increases first and then decreases with the increase of the doping amount of  $\text{Sm}_2\text{O}_3$ , especially at the sintering temperature of  $1330^\circ\text{C}$  and the doping amount of  $0.4\%$  reaches the maximum. Watanabe<sup>[17]</sup> believes that there are three stages in the replacement sequence of rare earth ions in the perovskite structure. The first two stages are rare earth ions to replace the A-site and B-site separately, and the third stage is that there would create a second phase when the doping content exceeds the ion of the solid solution limit. It can be inferred that during the period of dielectric constant growth,  $\text{Sm}^{3+}$  first enters the A-site to be substituted. Since the radius of  $\text{Sm}^{3+}$  is smaller than the radius of  $\text{Ba}^{2+}$ , so that lattice contraction will be caused and the crystal grains become smaller as can be seen in SEM images, and the internal stress is caused Lattice distortion, cell constant decreases, the dielectric constant increases. As a result of internal stress lead to lattice distortion, cell constant decreases. And the unit cell will produce barium ion vacancies, and produce a certain amount of electrons. The excess of a dielectric electron is captured by adjacent  $\text{Ti}^{4+}$  reduced to  $\text{Ti}^{3+}$ . These electrons are influenced by the spontaneous polarization field will be far from its balance Position, and produce a strong electron displacement polarization, and overlay with the spontaneous polarization field, enhanced ferroelectric, so that the dielectric constant increases. As shown in Eqs.(4):



When the doping amount of  $x(\text{Sm}_2\text{O}_3) > 0.4\%$ ,  $\text{Sm}^{3+}$  will gradually enter into the B-site to replace. In order to maintain the balance of the electricity price, some oxygen vacancies are

generated at the same time. Resulting in low dielectric constant because of the existence of "pinning effect"[18]. As shown in Eqs.(5):

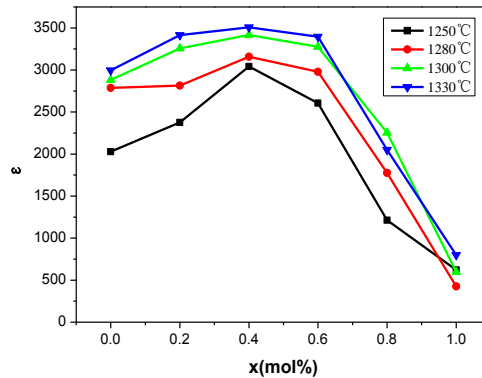


Fig.3. Dielectric constant of  $\text{Sm}_2\text{O}_3$  doped with BTS at room temperature.

It can be seen from the Fig. 4 that the dielectric loss of ceramics samples shows the trend of decreasing first, then increasing, then decreasing with the increase of  $x$  ( $\text{Sm}_2\text{O}_3$ ) doping amount. At  $x(\text{Sm}_2\text{O}_3)=0.40\%$ , the dielectric loss of each group of samples is at a minimum. When  $\text{Sm}^{3+}$  doping amount is small,  $\text{Sm}^{3+}$  replaces  $\text{Ba}^{2+}$  in A-site, and due to  $r(\text{Sm}^{3+}) < r(\text{Ba}^{2+})$ , the unit cell shrinks and the unit cell structure density increases, thus the dielectric loss decreases. In the other hand, there will produce electrons to make the system price to be compensated when the  $\text{Sm}^{3+}$  ions into the A-site, and the emergence of electrons will make  $\text{Ti}^{4+}$  reduced to  $\text{Ti}^{3+}$ , causing the sample dielectric loss increases. With the increase of  $\text{Sm}^{3+}$  doping amount,  $\text{Sm}^{3+}$  replaces  $\text{Ti}^{4+}$  at B-site. At the same time, The reduction of  $\text{Ti}^{4+}$  to  $\text{Ti}^{3+}$  is suppressed because of the occurrence of oxygen vacancies, resulting in a decrease in dielectric loss. Therefore, adding appropriate amount of  $\text{Sm}^{3+}$  into BTS can effectively reduce the dielectric loss.

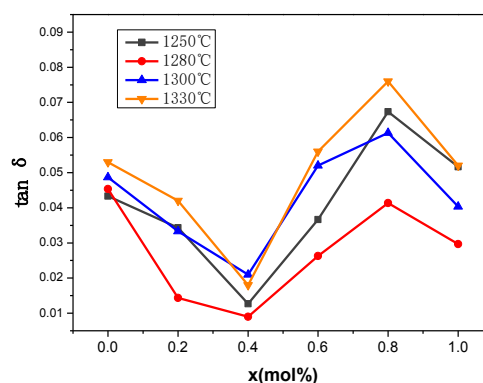


Fig. 4. Dielectric Loss of  $\text{Sm}_2\text{O}_3$  doped with BTS at room temperature.

Fig. 5(a), (b) shows the temperature dependence of dielectric constant and tangent loss for the samples at 1 kHz at 1330 °C for 2 h.

As shown in Fig. 5(a), with the increase of temperature the dielectric constant of each group of samples decreases. With the increase of doping amount, the peak value of dielectric constant of the sample first increases and then decreases gradually. This is related to the substitution mechanism of  $\text{Sm}^{3+}$  in the system. When the doping amount is less than 0.6%,

$\text{Sm}^{3+}$  mainly into the A-site to replace, which enhances the ferroelectricity of the sample. It is indicated that the appropriate amount of doped  $\text{Sm}_2\text{O}_3$  has certain has a peak effect, which increases the dielectric peak value of the ceramic sample. However, the Curie peak shift phenomenon is not obvious. The Curie temperature is always around 0 °C, so the doped of  $\text{Sm}_2\text{O}_3$  has little effect on the Curie peak of the sample. It can be seen from Fig. 5(b) that the dielectric loss of most of the samples shows a decreasing trend with the increase of the temperature as a whole, and gradually stabilized after the temperature exceeds 50 °C. And excessive doping of  $\text{Sm}_2\text{O}_3$  caused the increase of dielectric loss of samples. Dielectric loss of the sample increased when excessive doping  $\text{Sm}_2\text{O}_3$ . In conclusion, the samples have lower dielectric loss and higher dielectric constant when the doping amount is less than 0.6mol%, and the samples have good dielectric properties.

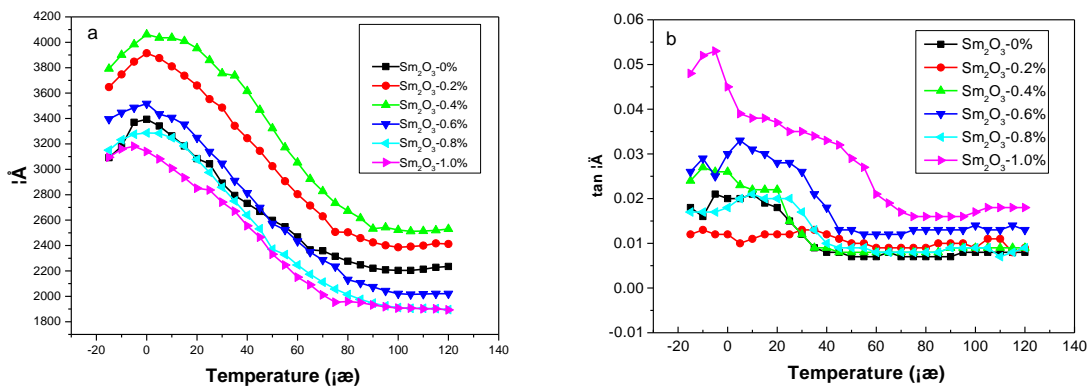


Fig.5. Temperature dependence of the dielectric constant and tangent loss of  $\text{Sm}_2\text{O}_3$  doped BTS ceramics.

#### 4. Conclusions

Ceramic samples of  $\text{BaTi}_{0.95}\text{Sn}_{0.05}\text{O}_3$  (BTS) were prepared by the conventional solid-state method using  $\text{BaCO}_3$ ,  $\text{SnO}_2$  and  $\text{TiO}_2$  as raw materials, and the influence of different doping amounts of  $\text{Sm}_2\text{O}_3$  addition on phase composition, microstructure and dielectric properties of BTS ceramics were investigated.

(1) By XRD diffraction image analysis, all doped BTS-based ceramic samples show a single perovskite structure, no other new phase formation.

(2) As shown in SEM images, a small amount of doped  $\text{Sm}_2\text{O}_3$  can refine grains to a certain extent and increase the density. When the sintering temperature is 1330°C and the content of  $\text{Sm}^{3+}$  is 0.4mol%, the structure density of the obtained sample is the best. With the further increase of doping amount, the porosity of ceramic samples gradually increases, and the existence of pores is not conducive to the dielectric properties of the samples.

(3) Appropriate amount of  $\text{Sm}_2\text{O}_3$  doping can significantly improve the dielectric constant of the BTS ceramic and reduce the dielectric loss. When the doping amount of  $\text{Sm}^{3+}$  ions is 0.4mol% and the sintering temperature reaches at 1330°C, the ceramic sample of the dielectric properties are optimized. Appropriate amount of doped  $\text{Sm}_2\text{O}_3$  also has a certain role in peak lifting, which increases the dielectric peak value of ceramic samples, but not obvious for the Curie peak shift.

#### Acknowledgements

This work was supported by Science and Technology Support Project of Hebei Province, China (Grant No. 15211111), and the National Natural Science Foundation of China (Grant No. 51502075).

## References

- [1] Nishino Atsushi, J. Power Sources **60**,137 (1996).
- [2] Chen Zhang, Yuanfang Qu, ShicaiMa, Materials Letters **61**,1007 (2007).
- [3] Chen Zhang, Yuanfang Qu, Transactions of Nonferrous Metals Society of China, **22**(11),2742 (2012).
- [4] L.Mitoseriu, V. Tura, C. Papusoi, T. Osaka, M. Okuyama, Ferroelectrics **223**,99 (1999).
- [5] Z. Yu, C. Ang, R. Guo, A.S. Bhalla, J. Appl. Phys. **92**,2655 (2002).
- [6] W.H. Payne, V.J. Tennery, J. Am. Ceram. Soc. **48**,413 (1965).
- [7] A. Chen, Y. Zhi, J. Zhi, Phys. Rev. B **61**,957 (2000).
- [8] J. Zhi, A. Chen, Y. Zhi, P.M. Vilarinho, J.L. Baptista, J. Appl. Phys. **84**,983 (1998).
- [9] X. Wei, Y.J. Feng, X. Yao, Appl. Phys. Lett. **83**,2031 (2003).
- [10] N.Horchidan, A. C.Ianculescu, L. P.Curecheriu, et al., Journal of Alloys & Compounds, , **509**(14), 4731 (2011).
- [11] X.Y.Wei, Y.J.Feng, X.Yao, Applied Physics Letters **83**,2031 (2003).
- [12] S.G. Lu, Z. K. Xu, H. Chena, Appl. Phys. Lett. **85**, 5319 (2004).
- [13] C. L. Tian, Z. X. Yue, Y. Y. Zhou, et al., J. Solid State Chem. **197**, 242 (2013).
- [14] D. Wang, R. Yu, S. Feng et al., Solid State Ionics **86**, 6335 (1999).
- [15] Chen Zhang, Zhi-xin Ling, Gang Jian, Fang-xu Chen, Transactions of Nonferrous Metals Society of China **27**, 2656 (2017).
- [16] B. D. Stojanovic, M. A. Zaghete, C. R. Foschini, F.O.S. Vieira, J. A. Varela, Ferroelectrics **270**, 15 (2002).
- [17] K. Watanabe, H. Ohsato, H. Kishl, et al. Solid State Ionics **108**(1/2/3/4), 129 (1998).
- [18] B. Su, T. W. Button, Journal of Applied Physics **95**(3),1382 (2004).